

Morphological Characterization of Bacteriogenic Manganese Oxides From Three Model Manganese (II/III) Oxidizing Bacterial Species

Wendy F. Smythe, Ph.D.

Michigan State University, BEACON Center for the Study of Evolution in Action

E-mail smythew@msu.edu

Abstract

Currently there is limited knowledge as to the morphology of bacteriogenic manganese (Mn)-oxide minerals, making it difficult to identify Mn minerals from geologic deposits as being biotic or abiotically formed. When investigating mineral deposits it is critical to understand what environmental processes lead to mineral formation in order to accurately interpret the information locked inside each mineral. This study aims to characterize the morphology, structural variability, and microbe-mineral association of bacteriogenic Mn(III/IV) oxides produced by Mn(II/III)-oxidizing bacteria, using pure cultures of three known Mn-oxidizing bacteria. Morphology and localization of bacteriogenic Mn-oxides was characterized using high resolution scanning electron (HR-SEM) and transmission electron microscopy (TEM). We found that the morphology of bacteriogenic Mn-oxides varies between bacterial species, and that the localization of Mn oxidizing enzymes determines if Mn-oxides are closely associated with the cellular surface or form in exopolysaccharides (EPS). Knowledge acquired from this study illustrates the complexity of identifying bacteriogenic Mn-oxides and oxidation products from more complex natural environmental settings like ancient geologic deposits.

Key words: biominerals, manganese oxides, biogenic manganese oxidation

Introduction

Mn-oxides are highly reactive minerals that play vital role in the biogeochemical cycling of elements, as they are naturally occurring strong oxidants, in addition they possess high sorptive capabilities that control the bioavailability of essential elements in the environment. Bacteria and some fungi are known to enzymatically catalyze the oxidation of soluble Mn(II/III) to Mn(III/IV) oxide minerals several orders of magnitude faster than abiotic Mn-oxidation, suggesting that most naturally occurring Mn-oxides are formed due to biogenic Mn-oxidation (19).

Bacteriogenic Mn-oxides, those produced exclusively by bacterium, possess novel nanosheet architectures exhibiting layer thicknesses from a few nanometers (nm) to hundreds of nm in lateral extent with organic material such as cellular structures and EPS serving as sites for mineral nucleation (3,19). These Mn-oxides possess increased surface areas, 98 to 224 m²/g, depending on bacterial species over synthetic δ -MnO₂, 39-98 m²/g,(18, 19, 20, 21). The goals of this study are to 1)

identify whether the morphology of the bacteriogenic Mn-oxides are a function of templating onto cellular surfaces, organic polymers, and 2) to determine whether bacteriogenic Mn-oxides are morphologically distinct from abiotic Mn-oxides much like bacteriogenic Fe(III) oxides are for bacterial species such as *Leptothrix* sp. which produce tubular stalks of Fe(III) oxides or *Gallionella* sp. which produce distinctive twisted stalks (7,14, 17) . To date there is no such body of knowledge available as to the morphology of biologically produced Mn-oxides our ability to distinguish biogenic from abiotic will allow us to better characterize Mn-oxides from ancient rock deposits and elucidate the role, if any, that microorganisms played in the formation of ancient deposits.

Morphological variability of bacteriogenic Mn-oxides was observed using three model bacterial species; *Pseudomonas putida* GB-1, *Bacillus* SG1, and *Erythrobacter* sp. SD21, each of which use a different mechanism for Mn-oxidation. Multicopper oxidase (MCO) and MopA enzymes that belong to a family of Ca²⁺-

binding heme peroxidases have been identified in several model Mn-oxidizing strains (2,13) and are thought to be the enzymes involved in bacteriogenic Mn oxidation. These enzymes oxidize a range of substrates through two one-electron transfers (2, 13, 16, 21).

Methods

Bacterial Strains

P. putida GB-1 is a gram-negative freshwater aerobic gammaproteobacterium isolated from sediments at the oxic/anoxic interface. This bacterium oxidizes Mn(II/III) to Mn(III/IV) with highest activity during early stationary phase, using both MCO associated with the cell wall and MopA, secreted into the surrounding environment where it may either localize with organic polymers or become loosely associated with the cellular membrane (2, 4, 10, 11).

Bacillus SG-1 a gram-positive marine Firmicutes that sporulates during stressful environmental conditions (i.e. nutrient deprivation). SG1 oxidizes Mn(II/III) using a membrane bound MCO within the exosporium (6, 8, 9, 12).

Erythrobacter sp. SD21 is a gram-negative strictly aerobic marine alphaproteobacterium isolated from surface sediments in San Diego Bay, this bacterium oxidizes Mn(II/III) using MopA (2).

Culture Conditions

In this study three Mn-oxidizing bacteria were grown in a controlled laboratory setting with a known concentration of Mn(II), in contrast to the natural environment where geochemistry changes rapidly altering the morphology and composition of Mn-oxides. Characterizations were done of microbe-mineral assemblages and of cleaned bacteriogenic Mn-oxides using electron microscopy. Cultures were grown in 500 ml flasks on shaker tables at 200 rpm for room temperature in Lept (GB1) or K medium (SG-1 and SD21) supplemented with MnCl₂ [Mn(II)] at a final concentration of 100 μM (5, 10, 11).

GB-1 and SD21 reach stationary phase and begin producing Mn-oxides within 30 hrs when grown at 32°C, for this study oxides were harvested after 2 days (2).

SG-1 spores were produced using a SG-1 plated colony to inoculate K sporulation medium amended with 100 μM Mn(II) (Dick et al., 2007). SG-1 reaches stationary phase within 24 hr and begins to sporulate and produce Mn-oxides within 7-10 days of incubation at 25°C.

Harvesting of Bacteriogenic Mn-Oxides

Once cultures reached stationary phase and Mn oxidation occurred Mn-oxides were harvested through a series of cleaning steps to remove organic material. Cultures were concentrated by centrifugation (Sorvall RT) at 684 g for 5 min at 4°C the supernatant was discarded leaving a pellet that was further cleaned to remove organics by suspension in 50 mL of the organic solvent hexane and vortexing for 1 min, pellets were allowed to settle for 5 min and then pelleted as before. Organic material extracted by the hexane wash remained suspended in solution and was decanted. The pellet is rinsed a second time in 50 mL of hexane with the addition of 1 mL of tetrahydrofuran (THF) to further dissolve organic material. The mixture was mixed on a vortex for 1 min, settled for 5 min and pelleted, after which the supernatant is again decanted, after which, Mn-oxides are rinsed a third time in 100% THF for 5 min, centrifuged and decanted as above. Mn-oxides are rinsed a final time in 100% acetone and processed as above and allowed to air-dry the overnight.

Microscopy

HR-SEM of Bacteriogenic Manganese Oxides

Morphology of microbe-mineral assemblages and cleaned bacteriogenic Mn-oxides were observed on an HR-SEM. Microbe-mineral assemblages were prepared by pipetting a 10 μL aliquot onto an aluminum pin and air-drying. Cleaned Mn-oxides were attached to aluminum

pins using carbon tape. All samples were coated with 20Å of gold using a Pelco 9100 (Ted Pella) sputter coater and observed on an FEI Siron HR-SEM (FEI, Hillsboro, OR) at the Portland State University Center for Electron Microscopy and Nanofabrication, Portland, OR. Specimens were observed at 3 kV with a working distance of 5.1 mm; digital images were captured.

Average measurements of Mn-oxides were taken using three digital images at the same magnification using ImageJ 1.49v image analysis and processing freeware (<http://imagej.nih.gov/ij/index>) (15).

TEM of Microbe-Mineral Assemblages

Whole mounts of microbe-mineral assemblages prepared for cryogenic TEM analysis were observed at the Environmental Molecular Sciences Laboratory at the Pacific Northwest National Laboratory in Richland, WA using an FEI high-resolution TEM, at 2 kV. Specimens were mounted on formvar coated, 300 mesh copper grids (Pelco) and air-dried. Specimens were observed in a natural hydrated state reducing dehydration artifacts. Specimens were pipetted (5 µL/grid) onto formvar-coated copper grids and prepared for cryofixation by plunging grids into liquid ethane using a Vitrobot; triplicates of each sample were prepared (1).

Ultra-thin sections of resin embedded specimens were observed for nano-scale cellular and mineralogical features on a Zeiss Libra 120 TEM (Carl Zeiss) at Delaware Biotechnology Institute BioImaging Center, Newark, DE. Samples were fixed in a 2% glutaraldehyde medium solution, after which samples were twice rinsed in 10 mM HEPES buffer pH 7.2 and dehydrated using a graded ethanol series (25%, 50%, 75%, 2x-100%). Samples were embedded in EMBED 812® (EMS, Hatfield, PA.) resin per manufactures instructions for medium resin and sectioned to 50-70 nm thickness using an ultra-microtome.

Results

Bacteriogenic Mn-oxides

Mn-oxides were found to possess a variety of morphologies as a function of the bacterial strain from which they were produced. Overall bacteriogenic Mn-oxides exhibited two morphologies that do not appear to be associated with the type of enzyme that forms the Mn-oxide.

Harvesting bacteriogenic Mn-oxides is a difficult process as EPS and exosporium are difficult to remove from the mineral surfaces. Following the cleaning step is essential to collective bacteriogenic Mn-oxides for characterizing morphology and for surface area measurements.

***Pseudomonas Putida* GB1**

HR-SEM analysis of Mn-oxides associated with *P. putida* GB1 which uses both MCO and MopA to oxidize Mn(II/III) to Mn(III/IV), exhibited a thin sheet like or platy morphology and appeared to be both incorporated into the cellular wall as well as in the EPS (Fig. 1A). Average thickness of Mn-oxides was 0.0413 nm. Cryogenic TEM of whole mounts showed nanoparticulate Mn-oxides associated with cellular surfaces (Fig. 1B).

Examination of ultra-thin sections on the TEM showed the same thin platy morphology and localization of bacteriogenic Mn-oxides associated with both the cell wall and EPS (Fig. 1C). EELS analysis coupled with false color overlays showed that minerals encrusting cell walls and EPS were Mn-oxides as indicated by distinctive spectral peaks at 644keV and 650keV indicative of Mn. (Fig. 1D-E).

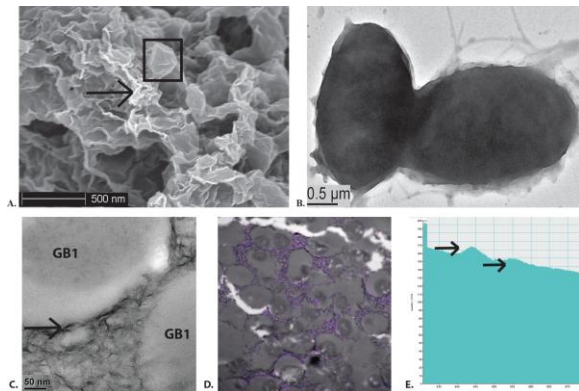


Figure 1. HR- SEM and TEM micrographs of *P. putida* GB-1. A) Low magnification HR-SEM illustrating the abundance of EPS (arrow) obstructing visualization of cells (box) and Mn-oxides. B) Cryogenic TEM showing Mn-oxides encrusting cell walls of GB-1 as evidenced by the increased contrast of cells. C) TEM of two cells with Mn-oxide plates closely associated with cell walls (arrow). D) False color overlay of Mn-oxides, purple indicates where Mn-oxides are present on cell walls and in EPS. E) EELS spectrum showing two Mn peaks at 644kV and 650kV (arrows).

Bacillus sp. SG1

The morphology of Mn-oxides produced in the exosporium of *Bacillus* SG-1 uses MCO to oxidize Mn(II/III) to Mn(III/IV) exhibited a “needle-like” morphology (Fig 2A). Mn-oxide Needles had a broad base at the exosporium surface that narrowed as oxides radiated outward away from the exosporium. Mn-oxides had an average diameter of 36.81 μm , and protruded on average 183.77 μm from the surface of the exosporium (Fig. 2B).

Cryogenic TEM of SG1 wet-mounts illustrates the direct association of Mn-oxides with the surface of the exosporium with Mn-oxide needles radiating from heavily encrusted spores (Fig. 2C).

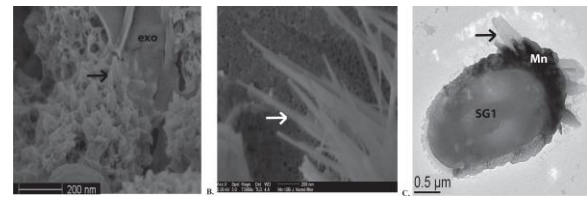


Figure 2. HR-SEM and cryogenic TEM micrographs of *Bacillus* SG1. A) HR-SEM of spores encrusted with Mn-oxide needles (arrow) forming in the exosporium (exo). B) Mn-oxide needles (arrow) illustrating how oxides taper as they grow out from the surface of the exosporium. C) Cryogenic TEM of spore (SG1) encrusted with Mn-oxides again illustrating the “needle-like” oxide morphology (arrow).

Erythrobacter SD21

The morphology of Mn-oxides produced by *Erythrobacter* sp. SD21 which uses MopA to oxidize Mn(II/III) to Mn(III/IV), demonstrated a rosette morphology comprised of stacked plates radiating from a central core (Fig. 3A-B). Mn-oxides appeared to be visually imperfect with a rugose texture and visible pore spaces. Mn-oxides averaged 903.9 μm x 1023.4 μm with a thickness of 21.59 μm . Plates were covered with pores that were between 4.3–18.39 μm with an average diameter of 11.81 μm .

Cryogenic TEM of SD21 showed the presence of Mn-oxides associated with both the cell wall and in the EPS. The cell wall was heavily encrusted with large platy Mn-oxides protruding from the cell surface (Fig.3C-D).



Figure 3. HR-SEM and TEM micrographs of Mn-oxides produced by *Erythrobacter* sp. SD21. A) Side view of Mn-oxide allowing for the observation of pore spaces (arrow) within the oxide. B) Top-down view of Mn-oxide, illustrating the rosette of large platy oxides radiating from a central core. C) Cryogenic TEM of Mn-oxides heavily encrusting a cell (white

arrow) and in the EPS (black arrow). D) Micrograph of large Mn-oxide plate.

Discussion

The morphology of bacteriogenic Mn-oxides was characterized using three known model Mn-oxidizing bacteria. Characterization was done using a variety of electron microscopy techniques, to better understand the microbe-mineral associations, structural variability, and localization of the bacteriogenic Mn-oxides. The goals of this study was to 1) identify whether the morphology of the Mn-oxide was a function of templating onto cellular surfaces, organic polymers, or merely a function of precipitation with no morphological affects to the Mn-oxides, and 2) do bacteriogenic Mn-oxides have a distinctive morphology that is easily identifiable from abiotic Mn-oxides, much like bacteriogenic Fe(III) oxides are. Findings suggest that there are multiple factors determining the localization of Mn oxidation on and around Mn-oxidizing bacteria. One factor is the presence and localization of the Mn-oxidizing enzymes, MCO and MopA, however, enzymes do not seem to influence Mn-oxide morphology.

In this study a robust cleaning step was developed to harvest bacteriogenic Mn-oxides free of organic material, EPS or exosporium. The cleaning step is essential to harvesting bacteriogenic Mn-oxides that can be used for morphological characterization, accurate surface area measurements or for acquiring an oxide to be used for further chemical reactions. Prior studies have found that MCOs have been found to catalyze Mn(II) oxidation on cell surfaces, resulting in encrustation of cells with Mn(III/IV) oxides (22). Here too we found that the model bacteria used to produce bacteriogenic Mn oxides, GB-1 and SG-1, resulted in the formation of and subsequent templating of Mn-oxides closely associated with the cell surface.

In contrast the Mn-oxidizing enzyme MopA is found both loosely associated with the cell wall and secreted into the surrounding environment (2, 10). Microorganisms, such as GB1 and SD21, that have MopA exhibit cell walls and EPS encrusted with Mn-oxides (11, 19).

EPS may serve as a nucleation site for Mn ions through the presence of reactive side chains that induce oxidation, from the presence of Mn oxidase enzymes embedded in the EPS matrix. We found that bacterial strains that produced more EPS or produced EPS more quickly demonstrated Mn oxidation sooner than bacterial strains that produced less EPS or produced EPS at a less rapid rate. However, we did not observe a change in the morphology of the Mn-oxides due the abundance of EPS or rate of Mn oxidation.

Bacteriogenic Mn-oxides demonstrated a broad range of morphologies beyond what we expected making it difficult to definitively identify bacteriogenic Mn-oxides in geologic deposits based on morphology alone. As we continue to characterize biogenic Mn-oxide morphology and better understand the mechanisms of Mn-oxidation we will better understand and be able to interpret the environmental and biological history of early Earth as we look through geologic history.

We do not yet fully understand how to influence the morphology of the bacteriogenic Mn-oxides, however one can speculate that chemical changes to the concentration of available Mn(II/III), or genetic studies to influence the expression of EPS or Mn oxidase genes may result in a Mn-oxide with a different morphology. As we continue to characterize bacteriogenic Mn-oxide morphology and the environments and conditions in which they form we will be better able to interpret the environments, microorganisms, and the

mechanisms that lead to Mn-oxide formation from ancient rock deposits.

Acknowledgements

This work was supported by the National Science Foundation (NSF), through grant DEB-1311616, the NSF GRFP and OCE-0424602. The author would like to thank Brad Tebo for serving as Ph.D. advisor, Alice Dohnokova and for her expertise and guidance preparing and analyzing cryogenic TEM specimens and the Environmental Molecular Sciences Laboratory for granting usage of their facilities. Thanks to Shannon Molda and Clara Chan from Delaware Biotechnology Institute, Bioimaging Center for assistance with TEM microscopy of ultra-thin sections. Thanks to Christina Butterfield and John Buzzo for providing bacterial strains for this study.

References

- Adrian, M., Dubochet, J., Lepault, J., McDowell, A.W. (1984). Cryo-electron microscopy of viruses. *Nature* 308 (5954): 32–36. <https://doi.org/10.1038/308032a0> PMID:6322001
- Anderson, C.R., Johnson, H.A., Caputo, N., Davis, R.E., Torpey, J.W. and Tebo, B.M. (2009). Mn(II) Oxidation Is Catalyzed by Heme Peroxidase in "Aurantimonas manganoxydans" Strain SI85-9A1 and *Erythrobacter* sp. Strain SD-21. *AEM*, Vol.75, No.12, p.4130-4138. <https://doi.org/10.1128/aem.02890-08>
- Bargar, J.R., Fuller, C.C., Marcus, M.A., Brearley, A.J., Perez De la Rosa, M., Webb, S.M., and Caldwell, W.A. (2009). Structural characterization of terrestrial microbial Mn oxides from Pinal Creek, AZ. *Geo Cos. Acta* 73, 889-910. <https://doi.org/10.1016/j.gca.2008.10.036>
- Brouwers, G.-J., J. P. M. de Vrind, P. L. A. M. Corstjens, P. Cornelis, C. Baysse and E. W. de Vrind-de Jong (1999). CumA, a gene encoding a multicopper oxidase, is involved in Mn²⁺-oxidation in *Pseudomonas putida* GB-1. *AEM* 65: 1762-1768.
- Dick, G.J., Torpey, J.W., Beveridge, T.J., and Tebo, B.M. (2007). Direct identification of a bacterial manganese (II) oxidase, the multicopper oxidase MnxG, from spores of several different marine *Bacillus* species. *AEM* 2008 Mar; 74(5):1527-34.
- Dick, G.J., Lee, Y.E., and Tebo, B.M. (2006). Manganese(II)-Oxidizing *Bacillus* Spores in Guaymas Basin Hydrothermal Sediments and Plumes. *AEM*, 72(5); 3184-3190. <https://doi.org/10.1128/AEM.72.5.3184-3190.2006>
- Fleming EJ, Cetinić I, Chan CS, Whitney King D, Emerson D. Ecological succession among iron-oxidizing bacteria. *The ISME Journal*. 2014;8(4):804-815. <https://doi.org/10.1038/ismej.2013.197>
- Francis, C.A., and Tebo, B.M. (2002). Enzymatic manganese (II) oxidation by metabolically dominant spores of diverse *Bacillus* species. *AEM* 68 (2):874-80. <https://doi.org/10.1128/AEM.68.2.874-880.2002> PMID:PMC126666
- Francis, C. A., and Tebo, B.M. (1999). Marine *Bacillus* spores as catalysts for oxidative precipitation and sorption of metals. *Journal of Molecular Microbiology and Biotechnology* 1: 71-78. PMID:10941787
- Geszvain, K., Smesrud, L., and Tebo, B.M. (2016). Identification of a Third Mn(II) Oxidase Enzyme in *Pseudomonas putida* GB-1. *AEM*, 13; 82(13):3772-82. <https://doi.org/10.1128/AEM.00046-16>
- Johnson, H.A. and Tebo B.M. (2008). In vitro studies indicate a quinone is involved in bacterial Mn (II) oxidation. *Arch. Microbiol*, 189: 59-60. <https://doi.org/10.1007/s00203-007-0293-y> PMID:17673976 PMID:PMC2721854
- Mandernack, K.W., Post, J., and Tebo, B.M. (1995). Manganese mineral formation by bacterial spores of the marine *Bacillus*, strain

SG-1: Evidence for the direct oxidation of Mn(II) to Mn(IV). *Geo. Cos. Acta* Vol. 59, I 21, pp. 4393-4408.

[https://doi.org/10.1016/0016-7037\(95\)00298-E](https://doi.org/10.1016/0016-7037(95)00298-E)

Nakama, K., Medina, M., Lien, a., Ruggieri, J., Collins, K., and Johnson, H.A. (2014). Heterologous Expression and Characterization of Manganese-Oxidizing Protein from *Erythrobacter* sp. Strain SD21. *AEM*, 80(21): 6837-6842.

<https://doi.org/10.1128/AEM.01873-14>

Pedersen, K. (2011). Gallionella. *Encyclopedia of Geobiology*. Pp 422-412. Springer Netherlands. Doi: 10.1007/978-1-4020-9212-1_96.

https://doi.org/10.1007/978-1-4020-9212-1_96

Schneider, C.A., Rasband, W.S., and Eliceriri, K.W. (2012). NIH Image to ImageJ: 25 years of image analysis. *Nature Methods* 9, 671–675 (2012) doi:10.1038/nmeth.2089.

<https://doi.org/10.1038/nmeth.2089>

Soldatova, A.V., Butterfield, C., Oyerinde, F., Tebo, B.M., and Spiro, T.G. (2012). Multicopper oxidase involvement in both Mn(II) and Mn(III) oxidation during bacterial formation of MnO₂. *JBIC: a publication of the Society of Biological Inorganic Chemistry*.

Suzuki T, Hashimoto H, Ishihara H, Kasai T, Kunoh H, Takada J. Structural and Spatial Associations between Fe, O, and C in the Network Structure of the *Leptothrix ochracea* Sheath Surface. *Applied and Environmental Microbiology*. 2011;77(21):7873-7875.

<https://doi.org/10.1128/AEM.06003-11>

Tebo, B.M., Clement, B.G., and Dick, G.J. (2007). Biotransformations of manganese. In: *Manual of Environmental Microbiology*, 3rd Edition, C.J. Hurst, R.L. Crawford, J.L. Garland, D.A. Lipson, A.L. Mills and L.D. Stetzenbach (Eds), ASM Press, Washington, D.C., pp. 1223-38.

<https://doi.org/10.1128/9781555815882.ch100>

Tebo, B.M., Bargar, J.R., Clement, B.G., Dick, G.J., Murray, K.J., Parker, D., Verity, R., and Webb, S.M. (2004). Biogenic Manganese Oxides: Properties and Mechanisms of Formation. *Annu. Rev. Earth Planet Sci.* 32: 287-328.

<https://doi.org/10.1146/annurev.earth.32.101802.120213>

Toner, B., Fakra, S., Villalobos, M., Warwick, T., and Sposito, G. (2005). Spatially Resolved Characterization of Biogenic Manganese Oxide Production within a Bacterial Biofilm. *AEM*, Vol. 71, No. 3, p. 1300-1310. doi: 10.1128/AEM.71.3.1300-1310.2005.

<https://doi.org/10.1128/AEM.71.3.1300-1310.2005>

Villalobos, M, Toner, B., Bargar, J., and Sposito, G. (2003). Characterization of the manganese oxide produced by *Pseudomonas putida* strain MnB1. *Geo. Cos. Acta*. Vol.67, N.14. p. 2649-62.

[https://doi.org/10.1016/S0016-7037\(03\)00217-5](https://doi.org/10.1016/S0016-7037(03)00217-5)

Zhang, A., Zhang, A., Chen, H., Liu, J., Liu, C., Ni, H., Zhao, C, Ali, M., Liu, F., and Li, L. (2015). Surface Mn(II) oxidation actuated by a multicopper oxidase in a soil bacterium leads to the formation of manganese oxide minerals. *Sci Reports* 5, Article: 10895, doi:10.1038/srep10895.

<https://doi.org/10.1038/srep10895>